SUPERNOVA REMNANTS AND MOLECULAR CLOUDS

J. Rho and W. Reach

SIRTF Science Center, California Institute of Technology, USA

RESUMEN

Revisamos observaciones en el cercano infrarrojo hechas recientemente con el *Observatorio Espacial Infrarrojo* (*ISO*) de un número de remanentes de supernova que están interactuando con nubes moleculares. Se detectaron las líneas de estructura atómica fina de [C II], [N II], [N III], [O I], [O II], [O III], [Si II], [P II], [Fe II], y dos líneas de hidrógeno molecular chocado, S(3) y S(9), para tres remanentes utilizando *ISO*. Se detectan casi todas las líneas atómicas. Ningun modelo de choque puede explicar todas las líneas observadas y para explicar las líneas detectadas se requieren densidades prechoque tanto moderadas ($10^2\,\mathrm{cm}^{-3}$) como altas ($\sim 10^4\,\mathrm{cm}^{-3}$). La alta densidad inferida y las temperaturas tibias provienen de grumos densos calentados por choques de supernovas, y los enfriadores principales de los choques radiativos son las líneas de [O I] a $63\,\mu$m y de [Si II] a $34.8\,\mu$m. También se detecta la emisión de H_2O, OH, y CO excitada por choques, lo cual es consistente con la excitación colisional en un gas muy denso ($2 \times 10^5\,\mathrm{cm}^{-3}$) y tibio. También tomamos imágenes del hidrógeno molecular y de [Fe II] por medio de observaciones terrestres, que revelan como se desarrollan los choques alrededor de las nubes. Se observan con mucha frecuencia los desplazamientos entre el hidrógeno molecular y las estructuras de [Fe II], y las imágenes muestran que está presente un solo choque principal a escalas grandes. Se discute la posibilidad de la formación estelar inducida por choques de supernova cuando éstos interactuan con las nubes.

ABSTRACT

We review recent *Infrared Space Observatory* (ISO) and near-infrared observations of a number of supernova remnants, which are interacting with molecular clouds. Atomic fine-structure lines of [C II], [N II], [N III], [O I], [O II], [O III], [Si II], [P II], [Fe II], and two lines of shocked molecular hydrogen S(3) and S(9), were detected for three remnants using *ISO*. Virtually all existing atomic lines are detected. No single shock model can account for all of the observed lines, and to explain the detected lines requires both moderate ($10^2\,\mathrm{cm}^{-3}$) and high ($\sim 10^4\,\mathrm{cm}^{-3}$) pre-shock densities. The inferred high density and warm temperatures are from heated dense clumps due to supernova shocks, and the principal coolants of radiative shocks are [O I] $63\,\mu$m and [Si II] $34.8\,\mu$m lines. Shock-excited far-infrared emission of H_2O, OH, and CO is also detected, which is consistent with collisional excitation in warm, very dense ($2 \times 10^5\,\mathrm{cm}^{-3}$) gas. We also took high-resolution images of molecular hydrogen and [Fe II] using ground-based observations, which reveal how shocks develop around clouds. Displacements between molecular hydrogen and [Fe II] structures are often observed, and the images show that a single primary shock is present on large scales. The possibility of star formation induced by supernova shocks when SN shocks interact with clouds is discussed.

Key Words: **MOLECULAR CLOUDS — STAR FORMATION — SUPERNOVA REMNANTS**

1. INTRODUCTION

Supernovae are believed to be the source of local kinetic energy of the interstellar medium, keeping the gas in motion and returning material from dense molecular clouds into the more diffuse interstellar medium and the galactic halo. Strong shock waves traversing the interstellar clouds compress, heat, chemically alter the medium, and trigger star formation. Despite the expected close association between Type II supernovae and molecular clouds, very few cases of supernova-molecular cloud interaction are known. The blast wave from a supernova within or near the edge of a cloud will progress rapidly through the inter-clump medium and drive slower shocks into dense clumps. Infrared lines are particularly useful diagnostics of supernova remnants in dense environments because infrared fine-structure lines are produced by dense gas expected behind radiative shocks and trace the ground-state populations of the all of the abundant elements.

2. FAR-INFRARED *ISO* SPECTROSCOPY

We obtained complete *ISO* LWS spectra of 1 position in the 3C 391, W 44, and W 28 supernova remnants as part of our program of observing supernova-molecular cloud interactions (Reach & Rho 1996, 1998). Figure 1 shows the *ISO* LWS spectrum from 42 to $188\,\mu$m for all three remnants. For each of the 10 LWS detectors, we removed the fringes using the *ISO* Spectral Analysis Package and subtracted a
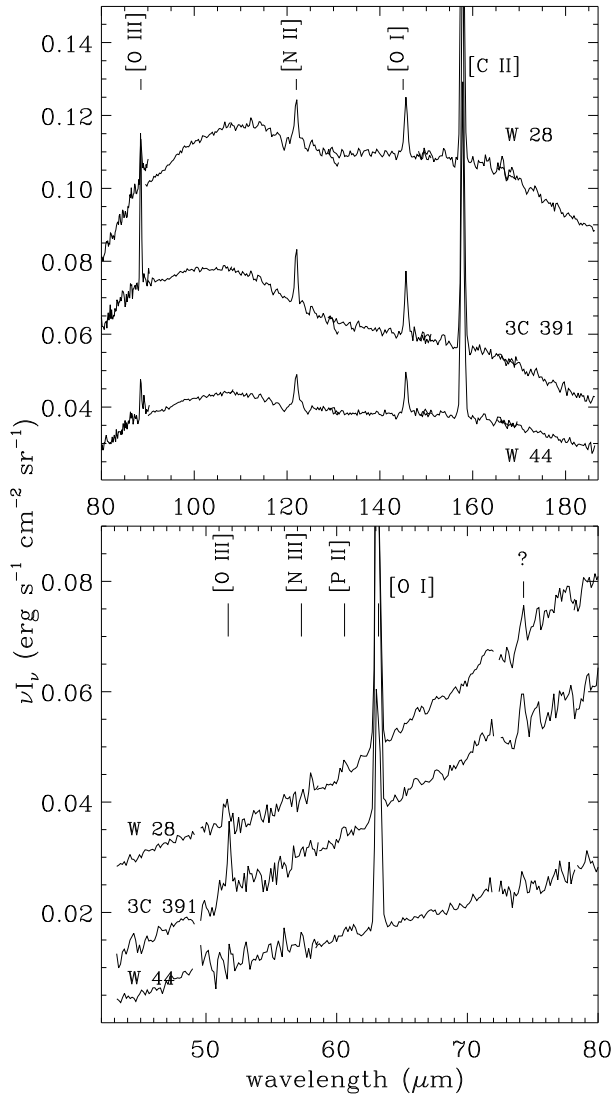
Fig. 1. LWS spectra of molecular shocks in the supernova remnants W 28, 3C 391, and W 44. The lower and upper panels show the wavelength ranges 42 to 80 and 80 to 187 μm, respectively. The bright atomic fine structure lines except [C II] are due to the remnants. From these spectra, we also detected weak molecular lines at long wavelengths, which is reported in Reach & Rho (1998).

constant (due to residual dark current). We detected atomic fine-structure lines from C^+, N^+, N^{++}, O^0, O^{++}, O^{+++}, and P^+ in the LWS spectra; all of the available ground-state fine-structure lines of the astronomically abundant molecules except Fe and Co lines are detected when we compare all possible fine-structure lines. The undetected ground-state lines are generally outside our wavelength range and for Fe and Co it is likely due to low abundances. Lines from high-ionization states were also not detected. Our own observations contain the wavelengths of 12
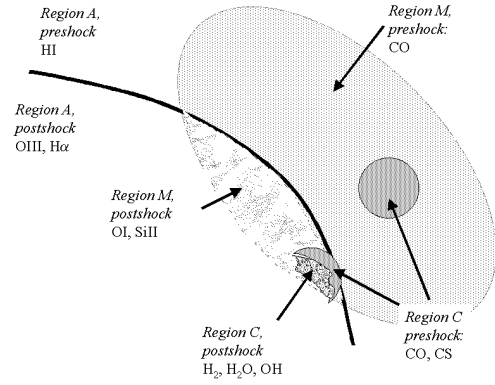

Fig. 2. Cartoon illustrating the different pre- and post-shock regions discussed in the paper. The physical properties of the regions are listed in Table 1. For each region, we also list an ion or molecule whose emission can be used to image the region.

fine-structure transitions among energy levels within 600 K of the ground state, from elements with abundance $> 10^{-7}$ relative to H in their expected ionization states. We detect essentially all of these lines, as well as lines from higher ionization states of the abundant elements: O III, O IV, and N III.

No single shock model can account for all of the observed lines. To determine the physical conditions where the lines are produced, and to determine the abundances of the elements in the shocked gas, we define three emitting regions based on the line diagnostics of detected lines. The Molecular region is the [O I], [Si II], [Fe II], and [N II] emitting region, with density, temperature, and column density set to give the observed brightnesses of the [O I] 63 and 145 μm lines. The Atomic region is the [O III] and [N III] emitting region, with density, temperature, and column density set to give the observed brightnesses of the [O III] 52 and 88 μm lines. Such a separation of emitting regions is anticipated because we expect that the neutral and doubly-ionized states of O would not be co-spatial—although there could, in principle, be overlap, if the gas is far from ionization equilibrium. The Clump region is a dense region that emits the CO, H_2O, OH, H_2 S(3) lines. Combining all of the constraints, we obtained the plausible range of density and temperature for Atomic, Molecular, and Clump regions, which is summarized in Table 1 and illustrated in Figure 2 (Reach & Rho 2000).

TABLE 1

PHYSICAL PROPERTIES OF THE THREE
POST-SHOCK EMITTING REGIONS

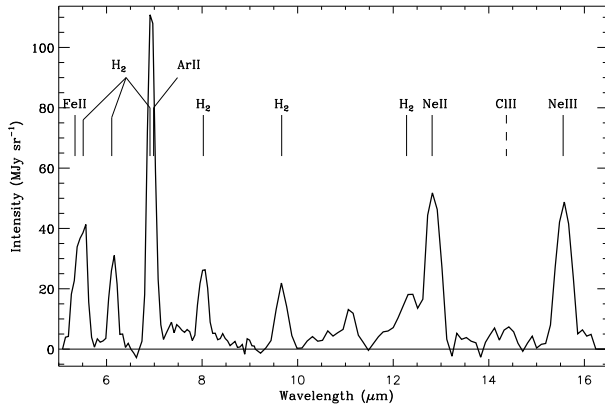|	pre-shock		post-shock	
Region	n_0 (cm^{-3})	V_s (km s^{-1})	n (cm^{-3})	T (K)
Atomic	< 1	500	8	3000
Molecular	10^2	100	3×10^3	600
Clump	10^4	20	4×10^5	200

Fig. 3. ISOCAM CVF spectrum of the molecular shock front 3C 391:BML. The spectrum is completely dominated by narrow emission lines: the continuum (and broad PAH features) are unrelated to the remnant. Each emission line is labeled with the ion or molecule that produced it.

3. MID-INFRARED *ISO* OBSERVATIONS

Observations of 3C 391 were made using the *Infrared Space Observatory* (Kessler et al. 1996) mid-infrared camera ISOCAM (Cesarsky et al. 1996) through a variety of filters. ISOCAM is a 32×32 pixel array, and we selected the $6''$ pixel field of view to get a large, un-vignetted field of view. First, on 1997 April 11, an image of the entire remnant was made in the wide LW3 (12 to $18\,\mu$m) filter.

We detected mid-infrared (12 to $18\,\mu$m) emission from 3C 391; the morphology is shell-like, similar to radio image of 3C 391. Having demonstrated that 3C 391 is a bright mid-infrared source, we returned to 3C 391 on 1997 November 3 to obtain a complete set of images with the circular-variable filter (CVF) from 5.14 to $16.14\,\mu$m. The mid-infrared spectrum of an ionic shock in 3C 391 can be separated from that of the molecular shock, because the molecular shock is spatially confined only to the 3C 391:BML region. Figure 3 shows an ISOCAM CVF spectrum, after
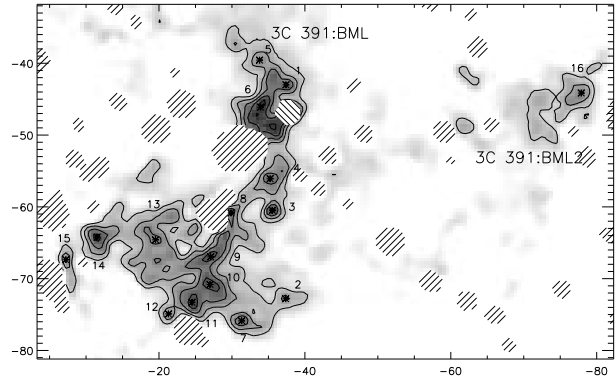

Fig. 4. Contour map of the continuum-subtracted H$_2$ image made with PFIRCAM. Contour levels range from 0.25 to $1.75 \times 10^{-4}\,\mathrm{erg\,s^{-1}\,cm^{-2}\,sr^{-1}}$. The coordinates are offsets, in arcsec, from ($18^\mathrm{h}49^\mathrm{m}24.8^\mathrm{s}$, $-00°56'31.1''$) (J2000). The H$_2$ clumps are labeled with numbers, and diagonal hatching indicates those positions containing stars.

subtracting the reference spectrum outside the remnant from the molecular region, which shows [Fe II], [Ar II], [Ne II], [Ne III], and a number of bright molecular hydrogen lines. When we compare this spectrum with the ionic shock region that is $1'$ away from the molecular region, we see that the ionic shock is completely different from the molecular shock, being dominated by the ionic lines.

4. NEAR-INFRARED HIGH-RESOLUTION IMAGING

We present new observations of the supernova remnant 3C 391 in the near infrared, using the H$_2$ $2.12\,\mu$m and [Fe II] $1.64\,\mu$m narrow-band filters in the Prime Focus Infrared Camera on the Palomar Observatory Hale 200 inch telescope, and in the mid-infrared (typical resolution of $1''$). The shocked H$_2$ emission is largely confined to the region 3C 391:BML ($40''$ size), where broad millimeter CO and CS lines had previously been detected. A small H$_2$ clump, $45''$ from the main body of 3C 391:BML, was confirmed to have broad CO emission, demonstrating that the near-infrared H$_2$ images can trace previously undetected molecular shocks. The [Fe II] emission has a significantly different distribution, being brightest in the radio bar and tracing the radio shell. The shocked molecular emitting region breaks up into a relatively structured, clumpy distribution. The H$_2$ emission is very clumpy, and all of the bright emission can be broken into 16 peaks as shown in Figure 4. H$_2$ emission reflects the distinct physical properties of the pre-shock gas. The shocks in 3C 391:BML are propagating into regions of much

higher pre-shock density, with $n_0 > 10^4 \, \mathrm{cm}^{-3}$. We estimated the mass from the observed brightness of the $2.12 \, \mu$m line using a 10-level model for the H_2 molecule over a range of densities and with kinetic temperature $1300 \, \mathrm{K}$ (derived in the next section); the mass of each clump ranges from 0.4 to $2 \, M_\odot$. We interpret these H_2 clumps as pre-stellar cores or possible protostars (Reach et al. 2002).

REFERENCES

Cesarsky, C., et al. 1996, A&A, 315, L32
Kessler, M. F., et al. 1996, A&A, 315, L27
Reach, W. T., & Rho, J. 1996, A&A, 315, L277
————. 1998, ApJ, 507, L93
————. 2000, ApJ, 544, 858
Reach, W. T., Rho, J., Jarrett, T. H., & Lagage, P.-O. 2002, ApJ, 564, 302

William Reach and Jeonghee Rho: Space Infrared Telescope Facility Science Center, California Institute of Technology, MS 220-6, Pasadena, CA 91125, USA (reach,rho@ipac.caltech.edu).